THE JOURNAL OF PHYSICAL CHEMISTRY B

Article

pubs.acs.org/JPCB

Chromophore Dynamics in the PYP Photocycle from Femtosecond Stimulated Raman Spectroscopy

Mark Creelman,[†] Masato Kumauchi,[‡] Wouter D. Hoff,[‡] and Richard A. Mathies*,[†]

[†]Department of Chemistry, University of California, Berkeley, California 94720, United States

[‡]Department of Microbiology and Molecular Genetics, Oklahoma State University, Stillwater, Oklahoma 74078, United States

Supporting Information

ABSTRACT: Femtosecond stimulated Raman spectroscopy (FSRS) is used to examine the structural dynamics of the *para*-hydroxycinnamic acid (HCA) chromophore during the first 300 ps of the photoactive yellow protein (PYP) photocycle, as the system transitions from its vertically excited state to the early ground state *cis* intermediate, I_0. A downshift in both the C_7═C_8 and C_1═O stretches upon photoexcitation reveals that the chromophore has shifted to an increasingly quinonic form in the excited state, indicating a charge shift from the phenolate moiety toward the C_9═O carbonyl, which continues to increase for 170 fs. In addition, there is a downshift in the C_9═O carbonyl out-of-plane vibration on an 800 fs time scale as PYP transitions from its excited state to I_0, indicating that weakening of the hydrogen bond with Cys69 and out-of-plane rotation of the C_9═O carbonyl are key steps leading to photoproduct formation. HOOP intensity increases on a 3 ps time scale during the formation of I_0, signifying distortion about the C_7═C_8 bond. Once on the I_0 surface, the C_7═C_8 and C_1═O stretches blue shift, indicating recovery of charge to the phenolate, while persistent intensity in the HOOP and carbonyl out-of-plane modes reveal HCA to be a cissoid structure with significant distortion about the C_7═C_8 bond and of C_9═O out of the molecular plane.

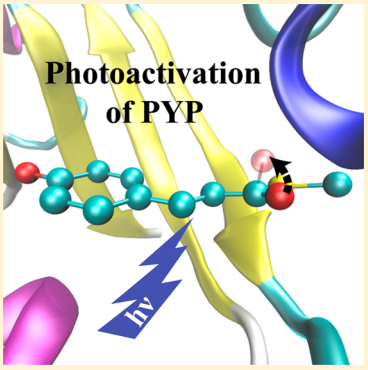

INTRODUCTION

Photoactive yellow protein (PYP) is a small (125 residue, 14 kDa) water-soluble protein isolated from the purple halophilic bacterium *Halorhodospira halophila*, where it serves as the photoreceptor for blue light avoidance. PYP owes its yellow color to a deprotonated *para*-hydroxy-cinnamic acid chromophore (HCA) covalently bound to Cys69 via a thioester linkage and non-covalently secured by extensive hydrogen bonding interactions (Figure 1). Absorption of blue light (λ_{max} = 446 nm) by the HCA chromophore initiates the PYP photocycle, which involves *trans*−*cis* isomerization about the C_7═C_8 bond within a few ps, protonation of the chromophore on the μs time scale, followed by partial unfolding of the protein and the exposure of the chromophore binding pocket in a few ms. The PYP_{dark} structure and protonation state are reformed in several hundred ms.[1−3]

The primary photochemistry of the PYP photocycle, from the initial excitation through the formation of the early *cis*-isomerized photointermediates, has been studied using a variety of ultrafast techniques on native PYP as well as PYP mutants and analogues. Fluorescence up-conversion established that the excited state of PYP (pG*) decays multiexponentially with time constants of ∼700 fs, ∼3−10 ps, and >100 ps, with the two fastest decay components ascribed to twisting of the chromophore about its vinyl bond.[4,5] Femtosecond IR studies on the early PYP photocycle show that charge translocation from the phenolate toward the ethylenic tail of HCA occurs in the pG* state along with the weakening of the H bond between

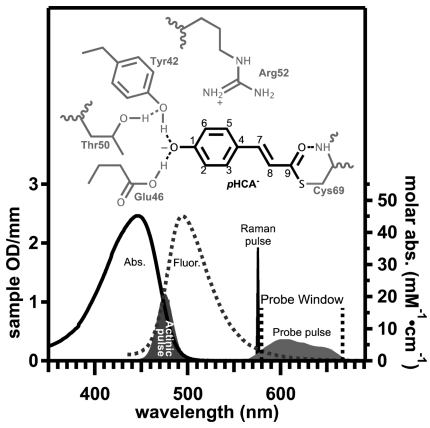

Figure 1. Structure of the *trans-p*-hydroxy-cinnamic acid PYP chromophore in the PYP_{dark} binding pocket. Optical parameters of the FSRS experiment are indicated over the PYP absorption (solid line, λ_{max} = 446 nm, ε_{446} = 45 500 M^{-1} cm^{-1}) and fluorescence spectra (dotted line, λ_{max} = 495 nm). The actinic pulse, which initiates the PYP photocycle, was tuned to 475 nm. The 575 nm Raman and 577−667 nm probe pulses lie in the red tail of the fluorescence band, and produce stimulated Raman spectra from 150 to 2200 cm^{-1}.

Received: August 27, 2013
Revised: November 13, 2013
Published: December 19, 2013

the HCA phenolate and Glu46.[6−8] UV ps Raman spectra of PYP also revealed changes in the hydrogen bonding between HCA and nearby protein residues, corroborating the weakening of the bond to Glu46 and showing that the H bond to Tyr42 is strengthened in the pG* state.[9] The Yoshizawa group published corroborating femtosecond Raman data from 800 to 1700 cm^{-1} where these shifts in the hydrogen bonding network were observed as early as 150 fs.[10] Recently, 8 fs pump−probe spectroscopy on the blue edge of the PYP absorption has revealed excited and ground state wave packets which suggest HCA adopts an increasingly quinonic form in its excited state, further supporting an excited state charge shift from the phenolate toward the ethylenic tail.[11] Femtosecond transient absorption (TA),[12−14] pump−probe IR[6,7] spectroscopies, and ultrafast transient absorption anisotropy measurements[15] have revealed the 3 ps formation of an early *cis*-isomerized, red-shifted (λ_{max} ∼ 510 nm) ground-state intermediate, I_0. Thus, the early stages of the photocycle involve a rapid change in the excited state hydrogen bonding network preceding the quenching of the excited state of the chromophore through a twisting motion, followed by the emergence of the isomerized ground state photoproduct species.

Pump-dump-probe experiments have been used to characterize the connectivity of excited and ground state intermediates and to explore the multiexponential decay processes that take place during the PYP photocycle. The data from these experiments can be interpreted through an inhomogeneous model or a homogeneous model. In the inhomogeneous model, structural inhomogeneity in the ground state leads to the population of several distinct excited states upon photoexcitation, each with a unique photoproduct yield. In the homogeneous model, the excited state population has a time-dependent yield and evolves on a complex, multidimensional potential energy surface with quenching pathways that compete with the photocycle.[16,17] These studies have also revealed the presence of a ground state intermediate (GSI) which results from unsuccessful attempts at photocycle initiation and leads back to the PYP_{dark} state. In addition, a multiphoton ionization pathway has been discovered which produces an ionized chromophore and solvated electron.[8,18]

The proposed mechanism for the ultrafast *trans*−*cis* isomerization of the HCA chromophore is through the out-of-plane rotation of the thioester linkage between HCA and the protein. This mechanism is essentially required as a result of the discovery by Xie et al.[19] that the phenolate moiety is held in place by hydrogen bonds during the isomerization.[7,19−21] At the thioester end of the HCA chromophore, the C_9═O carbonyl is hydrogen bonded to the protein backbone of Cys69, while the phenolate end of HCA is held in place by hydrogen bonds between C_1−O^- and Tyr42, Glu46, and Thr50 (Figure 1).[20] While the hydrogen bonds to the phenolate oxygen are conserved during the initial *trans*−*cis* isomerization, the hydrogen bond between the C_9═O carbonyl and Cys69 is broken in this process.[6−8,20,21] These observations have led to the conclusion that the carbonyl group rotates out of the plane of the chromophore while the phenolate moiety remains static during the early stages of C_7═C_8 photoisomerization.

To learn more about the chromophore structure and dynamics during the primary stages of the PYP photocycle, we turn to femtosecond stimulated Raman spectroscopy (FSRS).[22] The FSRS technique has been invaluable in studying the structural dynamics of photochemical processes including charge transfer[23,24] and ultrafast isomerizations occurring in protein systems,[25−28] owing to its high structural (∼20 cm^{-1}) and temporal (∼50 fs) resolution, along with its ability to selectively enhance scattering from specific chromophore groups. High time resolution allows FSRS to track the structural details of nonstationary states in ultrafast photoreactions.[28] Structural changes along the reaction coordinate are revealed through frequency shifts observed in the time-resolved FSRS spectra. Finally, it is advantageous to implement the FSRS technique because TA and vibrational spectra are simultaneously acquired, allowing for direct association between structural dynamics and electronic transitions.

The FSRS study presented here provides high-quality time-resolved structural data over the first 300 ps following PYP photoexcitation, including the pG*, I_0, and I_1 intermediates. By extending the probed window down to 350 cm^{-1} and following the reaction for several hundred ps with improved time resolution, we are able to present a detailed analysis of structurally important, low-frequency modes, in addition to correlating the FSRS data with simultaneously collected transient absorption spectra. This work reveals the ultrafast dynamics of the C_1═O, C_9═O, and C_7═C_8 bond strengths and out-of-plane distortion on the initially formed excited state and in the transition from the excited state to the photoproduct ground state providing a clearer picture of the mechanism of photoactivation in PYP.

EXPERIMENTAL METHODS

PYP was prepared as described previously[29−31] and in the Supporting Information. Briefly, apo-PYP of *Halorhodospira halophila* was expressed in *E. coli* and extracted with 8 M urea. Holo-PYP was reconstituted in 4 M urea by the addition of *p*-coumaric anhydride. The PYP was purified using column chromatography (DEAE-sepharose) and concentrated for analysis with ultrafiltration membranes. For FSRS experiments, the protein was concentrated to 0.75 OD/mm at 475 nm in a 10 mM Tris buffer (pH 7.0, 5% glycerol). This sample was circulated through a 1 mm path length optical flow cell (Starna, 48-Q-1). Sample integrity was confirmed with UV−vis before and after experiments.

The FSRS instrument has been described in detail elsewhere.[22,32] In brief, a 1 kHz regenerative Ti:sapphire amplifier (Spectra-Physics, Spitfire, ∼900 μJ pulses at 800 nm) with a duration of ∼150 fs is used to generate the three pulses necessary for FSRS, which are presented along with the absorption and fluorescence spectra of PYP in Figure 1. The actinic pulse (475 nm, 890 cm^{-1}, 30 fs, 300 nJ/pulse) was generated using a home-built non-collinear optical parametric amplifier (NOPA).[33] The Raman pulse (575 nm, 25 cm^{-1}, ∼590 fs, 300 nJ/pulse) was produced using a home-built narrow band OPA.[34] The continuum probe pulse (577−677 nm, ∼30 nJ/pulse) was generated by focusing a small portion of the fundamental into a sapphire plate. This continuum was compressed in a BK7 prism pair and used to stimulate the Stokes Raman transitions. All powers quoted are measured at the sample. The 90 fs temporal instrument response was measured using the optical Kerr effect between the actinic and probe pulses in the sample buffer and cell (Figure S1, Supporting Information).[35] The actinic pulse duration was determined by measuring the autocorrelation signal in 0.2 mm BBO. The Raman pulse bandwidth and duration were determined from the line widths of the cyclohexane Raman signals (assuming a transform limited pulse). Cyclohexane was

dx.doi.org/10.1021/jp408584v | J. Phys. Chem. B 2014, 118, 659−667

also used as the standard for Raman shift calibration. The three pulses are non-collinearly focused onto the sample using a 100 mm focal length achromatic lens. After passing through the sample, actinic and Raman pulses are blocked by an aperture, while the probe pulse is re-collimated with a 100 mm lens and focused into a spectrograph (Spex 500, 600 gr/mm, 500 nm blaze) and dispersed onto a front-illuminated CCD (Princeton Instruments, Pixis 100F). The CCD is synchronized to the 1 kHz amplifier pulse train so that each pulse can be read out separately. Phase-locked chopping of the Raman pulse at 500 Hz, and the actinic pulse at 250 Hz, allows for collection of the dark-state and photoexcited FSRS spectra as well as transient absorption in the probe window for a given delay time in four laser shots (4 ms) (Figure S2, Supporting Information).[24]

Time-resolved FSRS spectra were collected by varying the time delay between the actinic pulse and the Raman/probe pulse pair using a computer controlled delay stage (Physik Instrumente, M-405). The displayed spectra are averages of several thousand laser shots. The general data analysis procedure is presented in Figure S3 (Supporting Information). The PYP_{dark} FSRS spectrum is produced by subtracting a scaled buffer spectrum and a small baseline from the raw dark state FSRS spectrum. To produce the time-resolved FSRS spectra of photoexcited PYP, each time point is corrected for transient Raman pump effects, solvent and PYP_{dark} contributions, as well as other transient effects such as electronic absorption and emission. Stimulated emission adds to the number of Raman pump photons, which is observed as a transient increase in the FSRS signal. To correct for this, each photoexcited time point is normalized by comparing the intensity of the 1641 cm^{-1} OH bending mode of water with the non-photoexcited spectrum. The PYP_{dark} and buffer signals are then subtracted from each normalized time point. This step removes the contribution from the buffer but results in negative features due to oversubtraction of the dark state signals. This oversubtraction, which is due to the depleted population of PYP_{dark} after photoexcitation, is corrected by the addition of a scaled, buffer-subtracted, PYP_{dark} spectrum to each time point. The scale factor used in the depletion correction is related to the recovery of the PYP_{dark} species after photoexcitation (Figure S4, Supporting Information). A broad featured baseline is then subtracted from each time point to highlight the transient Raman bands of the photoexcited species. Kinetic analysis is performed by fitting FSRS peaks to Gaussian line shapes. The time evolution of the resulting frequencies and amplitudes are then fit to exponential functions convoluted with the 90 fs instrument response function.

RESULTS

Transient absorption (TA) data on PYP collected in the 578–665 nm probe window are presented in Figure 2. The top panel (A) displays selected wavelength resolved spectra of photoexcited PYP, from 200 fs to 300 ps. At early times (<1 ps), the ΔA spectra exhibit a large stimulated emission feature attributed to pG* at wavelengths shorter than ~645 nm and a small positive feature assigned to solvated electron generation due to photoionization at longer wavelengths. Though it has been previously reported that the photoionization pathway is inaccessible with 470 nm actinic pulses,[16] the assignment was confirmed by the observation of a quadratic dependence of the red absorption on the power of the actinic pulse. The strong stimulated emission (SE) feature from pG* decays rapidly, leaving a small emission signal at wavelengths shorter than 595

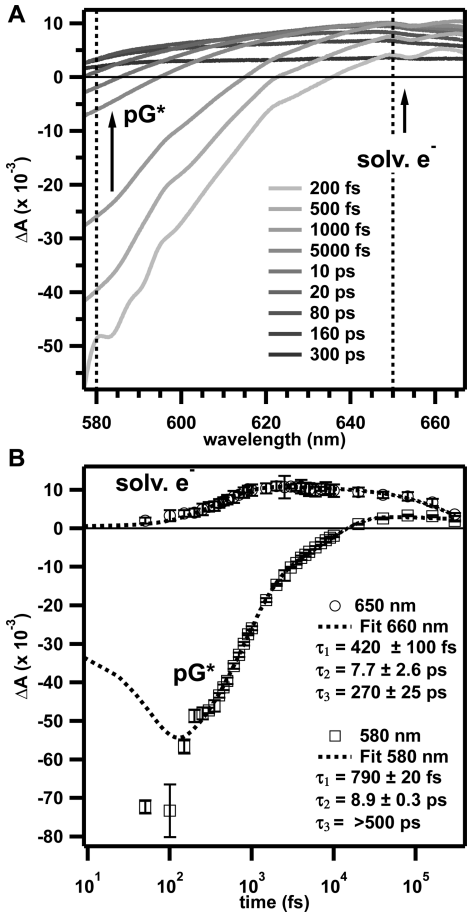

Figure 2. Transient absorption of PYP in the 577–677 nm probe window. (A) Selected transient absorption difference spectra from −2000 to 300 ps. (B) Kinetic data and fits for 580 nm (squares) and 650 nm (circles). Time constants for the fits are noted in the bottom panel.

nm after 5 ps. By 20 ps, all of the SE has decayed and the ΔA is small and positive over the entire probe window. The absorption feature, observed for wavelengths greater than 645 nm at early times, increases for the first several ps. After ~5 ps, the absorption signal begins decaying and continues to diminish for the duration of the experiment as the solvated electron and radical chromophore recombine.

Kinetic analysis of the TA features of pG* and the solvated electron are plotted as a function of time on a log scale in Figure 2B. The 580 nm SE feature due to pG* decays with a time constant of τ_1 = 790 ± 20 fs, eventually transitioning into an absorption signal (τ_2 = 8900 ± 300 fs) after ~20 ps. This 580 nm absorption feature decays slowly, but not entirely (τ_3 > 500 ps) through 300 ps, the longest delay time recorded. The solvated electron absorption feature at 650 nm initially grows in with a time constant of 420 ± 100 fs and reaches a maximum at ~2 ps, after which the signal decays on the multi-picosecond time scale (τ_2 = 7.7 ± 2.6 ps, τ_3 = 270 ± 25 ps). At 300 ps, the ΔA spectrum remains slightly positive over the entire probe window. While the time constants of the transient absorption are unaffected by the presence of the Raman pump, the amplitudes of the early decay and rise of the SE at 580 nm and the TA at 650 nm, respectively, are diminished, indicative of dumping of the excited pG* population by the Raman pump. The amplitude of the fast decay of the SE signal at 580 nm is

dx.doi.org/10.1021/jp408584v | J. Phys. Chem. B 2014, 118, 659–667

decreased by 20%, and the fast rise in the solvated electron TA at 650 nm decreases by nearly 60% in the presence of the Raman pump (Figure S5, Supporting Information).

The FSRS spectrum of PYP_{dark} presented at the bottom of Figure 3 corresponds well with previously published resonance

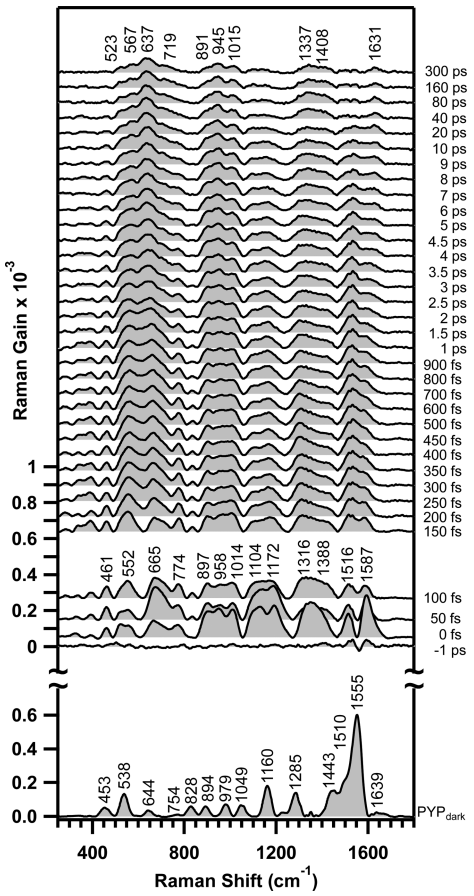

Figure 3. FSRS spectra of the *p*-hydroxy-cinnamic acid chromophore in PYP. The PYP_{dark} FSRS spectrum is displayed at the bottom. The time-resolved data from 0 fs to 300 ps are displayed above PYP_{dark} for comparison.

Raman spectra of the *p*-hydroxy-cinnamic acid chromophore.[21,36−38] However, due to the ∼25 cm^{-1} bandwidth of the Raman pulse, close lying features are not resolved in the FSRS spectra. The following mode descriptions are based on the assignments of Unno et al.[38] and described here according to their major character. The intense ethylenic mode at 1555 cm^{-1} is assigned to $C_7{=}C_8$ stretching coupled with the phenolate stretch analogous to the Y19a mode of tyrosine, while the shoulder at 1639 cm^{-1} is assigned to $C_9{=}O$ stretching. The bands at 1285, 1443, and 1510 cm^{-1} are all attributed to various CC vibrations of the aromatic ring; the 1285 and 1510 cm^{-1} modes are also coupled to the $C_7{=}C_8$ stretch. The 1160 cm^{-1} mode is the hydrogen in-plane bending vibration of the ring CH bonds. The 1049 cm^{-1} mode is assigned to the $C_8{-}C_9$ stretch. The $C_7H{=}C_8H$ and ring C—H hydrogen out-of-plane (HOOP) wagging vibrations are observed at 979 cm^{-1}. The 894 cm^{-1} band is assigned to bending of the carbon chain ($C_7C_8C_9$). The 828 cm^{-1} band is assigned to CC ring torsion and stretching. The 754 cm^{-1} mode is primarily due to the $C_9{=}O$ in-plane bend coupled with ring CC and $C_1{-}O$ stretching. The mode observed at 644 cm^{-1} is primarily due to the $C_9{=}O$ carbonyl out-of-plane vibration. The peaks at 453 and 538 cm^{-1} are attributed to in-plane vibrations and deformations of the ring and $C_7C_8C_9$ tail.

The structural dynamics of the first 300 ps of the PYP photocycle are presented as a stacked plot of the time-resolved FSRS spectra in Figure 3. Raman data of photoexcited PYP in the 800−1700 cm^{-1} spectral region are generally consistent with FSRS data obtained during the first ps of the photocycle presented by Nakamura et al.[10] though intensities differ slightly. Upon photoexcitation, a vibrational spectrum featuring several moderate intensity bands from 900 to 1600 cm^{-1} and a set of somewhat weaker bands between 400 and 800 cm^{-1} appears. These new features are readily observable after excitation, as their magnitudes are close to those observed for PYP_{dark}. Use of a 575 nm Raman pump pulse resulted in stokes FSRS spectra with negligible dispersion at early times, consistent with the findings of Nakamura et al. For the first 50 fs after excitation, the observed intensities fluctuate. These fluctuations may arise from rapid evolution on the excited state surface; however, they may also be due to artifacts created by the actinic pump, which is still impinging on the sample during this time. By 100 fs, a spectral pattern that smoothly evolves through 300 ps is apparent. Linearity of the power dependence of transient Raman signals has been confirmed, indicating they arise from photocycle intermediates arising from a single-photon pathway. Further, the 350 nm absorption of the radical, photoionized PYP[16] would gain little enhancement from the 575 nm Raman pulse, and is not expected to scatter strongly under the experimental conditions.

Because stimulated emission is observed during the first 10 ps after photoexcitation, Raman features observed during this time may be assigned partially to the decaying excited state, and will naturally contain the largest excited state contribution immediately following photoexcitation. The frequencies observed at early times are labeled in the 100 fs spectrum. Tentative assignments of these modes are made based on their proximity to dark state vibrational frequencies, and described according to their major contributing characters.[38] The peaks at 1516 and 1587 cm^{-1} fall in the region assigned to the $C_7{=}C_8$ stretch coupled with vibrations of the phenolate ring. However, the blue shift of the 1587 cm^{-1} shoulder to 1631 cm^{-1} by 300 ps suggest that this peak is likely associated with the $C_9{=}O$ stretch that downshifts from 1639 cm^{-1} in PYP_{dark}.[21] The peaks at 1316 and 1388 cm^{-1} appear in a region relatively unpopulated by dark state signals. The 1316 cm^{-1} mode is assigned to hydrogen in-plane wagging on $HC_7{=}C_8H$, which occurs at 1325 cm^{-1} in PYP_{dark}.[38] On the basis of its relatively large intensity, the 1388 cm^{-1} peak may be due to hydrogen in-plane bending and C—C stretching on the phenolate ring, which are seen at 1443 cm^{-1} in PYP_{dark}. However, the $C_1{-}O$ stretch has been calculated[38] to fall between 1300 and 1400 cm^{-1} and increased intensity in this region may also be due to increased polarizability of this bond following photoexcitation. The peaks at 1104 and 1172 cm^{-1} are likely due to hydrogen in-plane rocking vibrations, though the 1104 cm^{-1} peak may also correspond with an upshifted $C_8{-}C_9$ stretch. The peak at 1014 cm^{-1} is tentatively assigned to in-plane deformation of the phenolate ring, although this peak also lies very close to the region assigned to various hydrogen out-of-plane (HOOP) modes. The peak at 958 cm^{-1} is assigned to HOOP vibrations of the $C_7{=}C_8$ moiety. Skeletal vibrations and modes of the ethylenic tail of the chromophore are found below 900 cm^{-1}.

dx.doi.org/10.1021/jp408584v | J. Phys. Chem. B 2014, 118, 659−667

Also found in this region is the C_9=O carbonyl out-of-plane vibration at 665 cm^{-1}.

Several trends are noticeable in the transient PYP spectra during the first picosecond following excitation. Many of the peaks continue to grow in from 200−500 fs after excitation, the most noticeable being those at 552, 665, 958, and 1516 cm^{-1}. After the first ∼500 fs, every peak is decaying except for the HOOP mode at 958 cm^{-1} which continues to gain intensity, and the 665 cm^{-1} C_9=O carbonyl out-of-plane mode which maintains much of its intensity. In addition to the intensities, the frequencies of certain bands are also evolving. The frequencies of the peaks at 1172, 958, and 665 cm^{-1} are all downshifting while the peak at 1516 cm^{-1} is upshifting during this time. The frequencies of both the 1316 and 1587 cm^{-1} bands also shift, but they downshift for the first ∼500 fs followed by an increase in frequency.

The spectra evolve over the next several picoseconds as most of the intensities decay. By 40 ps, the intensity of the 1516 cm^{-1} peak as well as the signals observed between 1100 and 1200 cm^{-1} have grown very weak. From 40 to 300 ps, the spectral pattern remains largely unchanged, save for a slight decrease in signal intensity. By 300 ps, most of the remaining intensity is observed between 500 and 750 cm^{-1}, the region assigned to skeletal modes and vibrations of the ethylenic tail. The next largest intensities are seen between 850 and 1050 cm^{-1} where HOOP vibrations are expected to occur. Intensity also remains at 1337 and 1408 cm^{-1}. A small peak is visible at 1631 cm^{-1}; this peak has blue-shifted from the 1587 cm^{-1} shoulder observed at 100 fs and is assigned to the C_9−O stretch. Recovery to PYP_{dark}, determined from analysis of Raman depletion signals, is presented in Figure S4 (Supporting Information). The depletion decays multiexponentially with time constants of 50 ± 20 fs, 8.0 ± 0.8 ps, and 900 ± 400 ps.

The amplitudes and frequencies for several key Raman bands are plotted as a function of time in Figure 4. The kinetics of these peaks, as well as those not featured in the figure, were fit to a multiexponential decay convoluted with the 90 fs instrument response. The kinetics were fit to a simple, linear model in order to highlight the time ordering of photocycle structural dynamics while remaining agnostic to the various connectivity schemes proposed for the PYP photocycle. Though the observed kinetics are complex, involving many bands evolving with several different time constants, global analysis of the data revealed that all of the FSRS kinetics are well fit using the following set of time constants: 170 ± 20 fs, 870 ± 90 fs, 2600 ± 150 fs, 14 ± 6.5 ps, 45 ± 9.6 ps, and ∼800 ps.

Looking at the amplitudes (Figure 4, left column), many different sets of dynamics are observed. The peaks at 1587 and 1316 cm^{-1} both decay with a 2600 fs time constant assigned to I_0 formation, followed by an ∼800 ps decay. The ∼800 ps decay component is shared by all of the FSRS amplitudes and is assigned to the loss of Raman enhancement as I_0 eventually decays to I_1, which absorbs maximally at 465 nm.[13] The peaks at 1516 and 1172 cm^{-1} also share a set of time constants, 170 fs, 14 ps, and ∼800 ps. While the 170 fs component corresponds to a growth at 1516 cm^{-1}, it corresponds to a decay at 1172 cm^{-1}. Because the 170 fs process occurs faster than the stimulated emission decay, it is assigned to excited state dynamics. The 14 ps process occurs on the same time scale as dark state recovery. The peaks at 958 and 665 cm^{-1} each undergo unique amplitude kinetics. The 665 cm^{-1} peak initially grows in on the excited state, with a time constant of 170 fs, after which it decays with the 2600 fs I_0 formation, and continues decaying during the transition to I_1. The 170 fs process is not observed for the peak at 958 cm^{-1}, which grows in with the 2600 fs I_0 formation, then decays with a 14 ps and an ∼800 ps time constant.

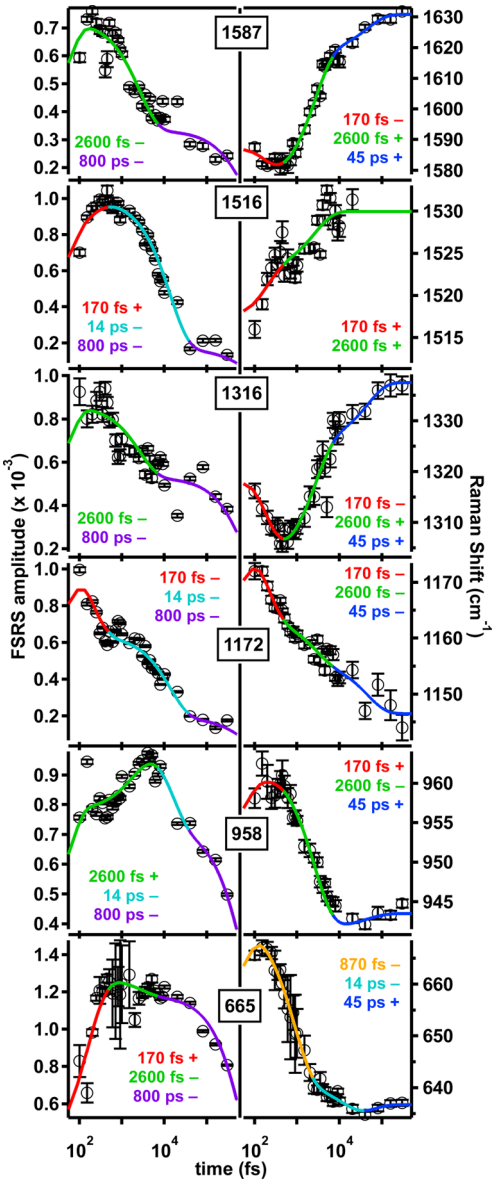

Figure 4. Kinetics of selected FSRS peaks. Time-resolved FSRS peaks were fit to Gaussian line shapes, and the resulting frequencies and amplitudes are plotted as a function of time above. The amplitudes are displayed in the left column, while the frequencies are displayed on the right. Peaks are labeled by their 100 fs frequency. The data have been fit to multiexponential functions convoluted with the 90 fs instrument response function. The kinetics are well fit using the following set of time constants: 170 ± 20 fs, 870 ± 90 fs, 2600 ± 150 fs, 14 ± 6.5 ps, 45 ± 9.6 ps, and ∼800 ps. Peaks are labeled with the relevant time constants. Rises and decays are indicated by + and − signs, respectively. The best-fit lines are color coded to indicate which time constant is describing the convoluted exponential function at a given time.

The frequency kinetics are more homogeneous, with most kinetics fitting to the three time constants: 170 fs, 2600 fs, and 45 ps. Shifts on these time scales reveal structural dynamics on the excited state, as well as those occurring during and

dx.doi.org/10.1021/jp408584v | J. Phys. Chem. B 2014, 118, 659−667

following I_0 formation. The kinetics for the peak at 1516 cm^{-1} do not include the 45 ps component, as this peak has virtually disappeared after 20 ps. The frequency of the peak at 665 cm^{-1} was found to shift with different kinetics than the other peaks, and is best fit using the time constants 870 fs, 14 ps, and 45 ps. The downshift of the 665 cm^{-1} peak could not be satisfactorily fit without the 870 fs component. These unique kinetics correspond well with the stimulated emission decay.

DISCUSSION

Previous studies, employing time-resolved absorption,[12−14] fluorescence,[4,5,39] Raman,[37,40] and IR[6−8] techniques, have revealed a basic picture of the primary photochemistry of PYP. The FSRS data presented in this paper affirm these previous studies and also offer new information on the structural dynamics during the transition from pG* to the early photoproduct I_0, particularly through the 200−800 cm^{-1} data. In order to visualize the key changes associated with the kinetic processes identified above, FSRS spectra corresponding with each kinetic intermediate are presented in Figure 5.

The FSRS spectra immediately following photoexcitation are strikingly different from the PYP_{dark} spectrum, featuring shifted frequencies and vastly different relative intensities. The early 100 fs species has been designated as the Franck−Condon excited state (FC*). Notably, peaks in the 400−700 cm^{-1} region have gained intensity at the expense of the large ring modes at ∼1550 cm^{-1}. The large relative intensities throughout the spectrum are indicative of broken symmetry. In particular, the HOOP intensity at 958 cm^{-1} is characteristic of distortion about the C_7═C_8 double bond. Large changes in both the dipole moment and polarizability of the photoexcited HCA chromophore have been previously observed using Stark-effect spectroscopy, indicating a charge shift in the excited state.[41] Redistribution of the negative charge from the phenolate oxygen of HCA to the carbonyl would be expected to enhance the polarizability, and hence the Raman intensities of modes localized on the ethylenic tail with the opposite being true for modes of the phenolate ring. This charge redistribution is also expected to alter certain frequencies as the structure becomes increasingly quinonic.[42] In the quinonic form, the C_7═C_8 and C_9═O bond orders should decrease while the C_4—C_7, C_8—C_9, and C_1—O^- bond orders should increase. This prediction is confirmed in the FC* spectrum (Figure 5) where the C_7═C_8 stretching dominated mode has downshifted to 1516 cm^{-1} and the C_9═O stretch has downshifted to 1587 cm^{-1}. The new peak at 1104 cm^{-1} could correspond with an upshifted C_8—C_9 stretch. The C_1—O stretch is very weak and not resolved in our PYP_{dark} spectrum but has previously been observed at 1343 cm^{-1}.[38] New intensity at 1390 cm^{-1} in the FC* spectrum may correspond to an upshifted C_1—O stretch, which would be expected to gain intensity with increasing double-bond character. The observed intensity and frequency changes in the 100 fs spectrum are consistent with a charge-shifted, distorted FC* state.

The FC* state then undergoes a transition with a time constant of 170 ± 20 fs that is significantly faster than the stimulated emission decay. This process is interpreted as excited state evolution from the initially formed FC* state to an increasingly charge shifted pG* as the chromophore nuclei respond to the instantaneous dipole change[41] induced by photoexcitation. During this transition, it is likely that the deprotonated chromophore settles further into the quinonic form, increasing localization of the charge on the C_9═O

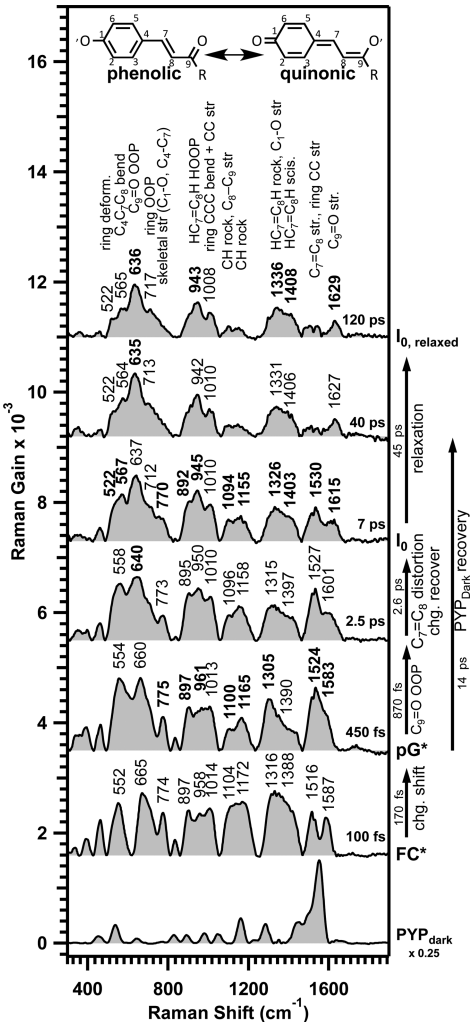

Figure 5. The FSRS spectra of observed kinetic intermediates. The 1/e time constant and the structural changes associated with each intermediate are indicated to the right of the spectra. The 120 ps spectrum is the average of the 80 and 160 ps time points; all other spectra correspond with the time points displayed in Figure 3. Bold labels indicate which frequencies have shifted concurrently with the formation of each intermediate. Mode character assignments are listed above the corresponding peaks.

oxygen.[42] Key structural changes occurring with pG* formation include a downshift of the C_9═O stretching frequency from 1587 to 1583 cm^{-1} consistent with the expected lowering of the C_9═O bond order in the quinonic form. The hydrogen in-plane vibrations observed at 1172 cm^{-1} in the excited state downshift to 1165 cm^{-1}, which may result from decreasing the bond order of the C_7═C_8 stretch but may also result from twisting of the H_7C═C_8H hydrogens out of the local plane. The frequency of the 1516 cm^{-1} mode also upshifts on this time scale to ∼1524 cm^{-1}; the indicated increase in the C_7═C_8 bond order would be inconsistent with increasing quinonic form of the chromophore. However, this mode is coupled to the C_2═C_3 and C_5═C_6 stretches in the ring, which would both be expected to increase in bond order upon a phenolic to quinonic transition. These observations indicate that initial movements from the FC* state are driven by a charge relocation which may prime the system for isomerization by lowering the C_7═C_8 bond order. The 450 fs FSRS spectrum of

dx.doi.org/10.1021/jp408584v | J. Phys. Chem. B 2014, 118, 659−667

the relaxed pG* state displayed in Figure 5 represents the completion of this process.

Following the excited state charge shift, the C_9=O carbonyl out-of-plane vibration at 665 cm^{-1} downshifts to 640 cm^{-1} with a time constant of 870 ± 90 fs. It has been previously demonstrated, based on ultrafast IR studies, that a requirement for successful entry into the PYP photocycle is the breaking of the hydrogen bond between C_9=O and Cys69.[8] Breaking or weakening of the hydrogen bond with Cys69 would be expected to reduce the restoring force, and thus lower the frequency of the C_9=O out-of-plane vibration, as observed, thus providing compelling support for these hypotheses. These kinetics closely match the previously observed 700 fs excited state decay[4,5,12,14] as well as the 790 fs stimulated emission decay reported here. The absence of a 700 fs decay component in studies on PYP assembled with locked chromophore analogues has led to the assignment of this kinetic process to twisting of the *p*-hydroxy-cinnamic acid chromophore.[4,5] We suggest that this out-of-plane motion of C_9=O is the initial trajectory leading to the ground state surface and successful entrance into the photocycle. The spectrum resulting from the completion of this process is represented by the 2.5 ps time point displayed in Figure 5. This spectrum likely also contains contributions from longer-lived excited state and ground state species not leading to the photocycle.

After the downshift of the C_9=O carbonyl out-of-plane vibration, many frequencies and intensities evolve with a 2.6 ± 0.2 ps time constant, in good agreement with the reported kinetics for the formation of the *cis* photoproduct, I_0.[13,14] The C_9=O stretch upshifts from 1583 to 1615 cm^{-1}, consistent with a return of the charge toward its dark state phenolic configuration. The frequency of the C_7=C_8 stretch + ring mode at 1516 cm^{-1} continues to upshift on this time scale to 1530 cm^{-1}. A downshift in the hydrogen in-plane region to 1155 cm^{-1} is likely due to further torsion along the C_7=C_8 bond, which relieves steric repulsions, allowing for lower frequency in-plane motion. This conclusion is further supported by the increase in the HOOP intensities and their downshift to 943 cm^{-1} on this time scale, indicating increased distortion of the C_7=C_8 bond and a twisted cissoid structure for I_0.

Following the formation of I_0, structural changes observed in the FSRS data are subtle, and are dominated by amplitude decay. A process occurring with a time scale of ~10 ps is observed in fluorescence decay, dark state recovery, and FSRS kinetics (8.9 ± 0.3, 8 ± 0.8, and 14 ± 6.5 ps, respectively). This process likely involves the return to the dark state from the previously identified GSI, whose lifetime has been reported as ~6 ps in addition to the longer lived, unproductive excited state population that has also been reported to fall back into the dark state.[8] This recovery occurs on the same time scale as an ~5 cm^{-1} downshift of the C_9=O carbonyl out-of-plane vibration from 640 to 635 cm^{-1}. Loss of Raman intensity from the GSI and excited state species as they return to the dark state configuration, leaving behind the cissoid, non-H-bonded photoproduct, may be expected to further reduce the overall observed frequency of the C_9=O carbonyl out-of-plane mode. The 40 ps spectrum in Figure 5 results from the completion of this recovery process. If this interpretation is correct, time points prior to 40 ps will contain vibrational features of both the excited state, ground state photocycle intermediates and GSI leading back to the dark state, while time points following 40 ps will be due primarily to photocycle intermediates.

The dark state recovery kinetics in Figure S4 (Supporting Information) show that ~15% of the excited molecules recover directly to the dark state within the first few hundred fs. By 20 ps, an additional 50% of dark state depletion has been filled in, leaving 35% of the initially excited population in the photocycle or photoionization pathway. Photoionization likely accounts for less than 5% of the photoexcited population due to the rather large absorptivity of the solvated electron.[43] A ~30% conversion efficiency from pG* to the ground state photoproducts is consistent with previous results.[12,44] In the first few ps, we observe a 75% decrease in the fluorescence signal, with the remaining 25% decaying by 20 ps.

Finally, frequencies are observed to slightly upshift with a 45 ± 9.6 ps time constant. This process is assigned to relaxation of the chromophore and protein in the I_0 state. A spectrum of this species is displayed as $I_{0,relaxed}$ in Figure 5. The remaining HOOP intensity at 943 cm^{-1} indicates that $I_{0,relaxed}$ is still highly distorted about the C_7=C_8 bond. This stored distortion energy may be mechanistically important because it can be used to drive later structural changes in the photocycle. The 45 ps relaxation of I_0 is followed by an amplitude decay with a time constant of ~800 ps as I_0 decays to I_1.

Recently, Schotte et al. published time-resolved Laue structures of the PYP photocycle taken with only 150 ps resolution. Their earliest recorded photointermediate crystal structure, which nominally corresponds to the two longest FSRS time points measured in our experiment, shows a distorted cissoid structure with the C_9=O carbonyl displaced ~90° out of the phenolate plane but still hydrogen bonded with Cys69.[45] While photocycle intermediates trapped in a crystal do not necessarily directly correspond with those observed in solution, it is clear that this crystal structure geometry would involve a weaker hydrogen bond between C_9=O and Cys69. Thus, both the Laue data and our observation of a reduced C_9=O out-of-plane vibrational frequency support a reduced hydrogen bond strength between C_9=O and Cys69 in $I_{0,relaxed}$.

CONCLUSIONS

In summary, we have observed the vibrational structural dynamics taking place during the early events of the PYP photocycle. This work provides new structural evidence for an excited state charge separation following the initial Franck–Condon excitation. The decrease in the C_9=O stretching frequency within 200 fs indicates an increase in the charge localization on the carbonyl, which results from the molecule adopting an increasingly quinonic form. The C_9=O carbonyl out-of-plane vibration downshifts from 665 to 640 cm^{-1} concurrently with the fastest observed fluorescence decay component (τ ~ 800 fs), indicating that this motion lies along the reaction coordinate leading out of the excited pG* state and into the photocycle. This downshift in the carbonyl out-of-plane vibration results from the loss of restoring force as the hydrogen bond between C_9=O and Cys69 is weakened, and eventually broken. Once on the photoproduct surface, increases in the C_9=O and C_7=C_8 stretching frequencies indicate a restoration of the phenolic bond ordering, and thus the return of the negative charge to the phenolate moiety. The persistence of intensity in the HOOP region indicates that following relaxation I_0 remains highly distorted about the C_7=C_8 bond. Relieving this distortion is a likely driving force for the remaining PYP photocycle.

These new time-resolved structural data support an isomerization mechanism whereby the C_9=O carbonyl rotates out of

dx.doi.org/10.1021/jp408584v | J. Phys. Chem. B 2014, 118, 659–667

plane, weakening its hydrogen bond with Cys69, and forming a distorted cissoid photoproduct intermediate, I_0, which likely stores energy used to further drive the photocycle. The data also provide insight into the role excited state charge shift plays in facilitating the carbonyl rotation, and thus entrance into the PYP photocycle.

■ ASSOCIATED CONTENT

Supporting Information

Detailed protein preparation methods and figures for instrument response measurement, pulse timing, data analysis, ground state recovery, and the effects of the Raman pump on transient absorption. This material is available free of charge via the Internet at http://pubs.acs.org.

■ AUTHOR INFORMATION

Corresponding Author

*E-mail: ramathies@berkeley.edu. Phone: 510-642-4192. Fax: 510-642-3599.

Notes

The authors declare no competing financial interest.

■ ACKNOWLEDGMENTS

We thank Sangdeok Shim for his laser expertise, David Hoffman for his contributions to the instrument and data analysis tools, and Rosalie Tran and Jyotishman Dasgupta for many helpful discussions. This work was supported by the Mathies Royalty Fund and NSF grant MCB-1051590 to W.D.H.

■ REFERENCES

(1) Cusanovich, M. A.; Meyer, T. E. Photoactive Yellow Protein: A Prototypic PAS Domain Sensory Protein and Development of a Common Signaling Mechanism. *Biochemistry* **2003**, *42*, 4759−4770.

(2) Hellingwerf, K. J.; Hendriks, J.; Gensch, T. Photoactive Yellow Protein, A New Type of Photoreceptor Protein: Will This "Yellow Lab" Bring Us Where We Want to Go? *J. Phys. Chem. A* **2003**, *107*, 1082−1094.

(3) Larsen, D. S.; van Grondelle, R. Initial Photoinduced Dynamics of the Photoactive Yellow Protein. *ChemPhysChem* **2005**, *6*, 828−837.

(4) Chosrowjan, H.; Mataga, N.; Nakashima, N.; Imamoto, Y.; Tokunaga, F. Femtosecond-Picosecond Fluorescence Studies on Excited State Dynamics of Photoactive Yellow Protein from Ectothiorhodospira Halophila. *Chem. Phys. Lett.* **1997**, *270*, 267−272.

(5) Changenet, P.; Zhang, H.; van der Meer, M. J.; Hellingwerf, K. J.; Glasbeek, M. Subpicosecond Fluorescence Upconversion Measurements of Primary Events in Yellow Proteins. *Chem. Phys. Lett.* **1998**, *282*, 276−282.

(6) Groot, M. L.; van Wilderen, L. J. G. W.; Larsen, D. S.; van der Horst, M. A.; van Stokkum, I. H. M.; Hellingwerf, K. J.; van Grondelle, R. Initial Steps of Signal Generation in Photoactive Yellow Protein Revealed with Femtosecond Mid-Infrared Spectroscopy. *Biochemistry* **2003**, *42*, 10054−10059.

(7) Heyne, K.; Mohammed, O. F.; Usman, A.; Dreyer, J.; Nibbering, E. T. J.; Cusanovich, M. A. Structural Evolution of the Chromophore in the Primary Stages of Trans/Cis Isomerization in Photoactive Yellow Protein. *J. Am. Chem. Soc.* **2005**, *127*, 18100−18106.

(8) Van Wilderen, L. J. G. W.; van der Horst, M. A.; van Stokkum, I. H. M.; Hellingwerf, K. J.; van Grondelle, R.; Groot, M. L. Ultrafast Infrared Spectroscopy Reveals a Key Step for Successful Entry into the Photocycle for Photoactive Yellow Protein. *Proc. Natl. Acad. Sci. U.S.A.* **2006**, *103*, 15050−15055.

(9) Mizuno, M.; Kamikubo, H.; Kataoka, M.; Mizutani, Y. Changes in the Hydrogen-Bond Network around the Chromophore of Photoactive Yellow Protein in the Ground and Excited States. *J. Phys. Chem. B* **2011**, *115*, 9306−9310.

(10) Nakamura, R.; Hamada, N.; Abe, K.; Yoshizawa, M. Ultrafast Hydrogen-Bonding Dynamics in the Electronic Excited State of Photoactive Yellow Protein Revealed by Femtosecond Stimulated Raman Spectroscopy. *J. Phys. Chem. B* **2012**, *116*, 14768−14775.

(11) Liu, J.; Yabushita, A.; Taniguchi, S.; Chosrowjan, H.; Imamoto, Y.; Sueda, K.; Miyanaga, N.; Kobayashi, T. Ultrafast Time-Resolved Pump−Probe Spectroscopy of PYP by a Sub-8 Fs Pulse Laser at 400 Nm. *J. Phys. Chem. B* **2013**, *117*, 4818−4826.

(12) Baltuska, A.; van Stokkum, I. H. M.; Kroon, A.; Monshouwer, R.; Hellingwerf, K. J.; van Grondelle, R. The Primary Events in the Photoactivation of Yellow Protein. *Chem. Phys. Lett.* **1997**, *270*, 263−266.

(13) Ujj, L.; Devanathan, S.; Meyer, T. E.; Cusanovich, M. A.; Tollin, G.; Atkinson, G. H. New Photocycle Intermediates in the Photoactive Yellow Protein from Ectothiorhodospira Halophila: Picosecond Transient Absorption Spectroscopy. *Biophys. J.* **1998**, *75*, 406−412.

(14) Devanathan, S.; Pacheco, A.; Ujj, L.; Cusanovich, M.; Tollin, G.; Lin, S.; Woodbury, N. Femtosecond Spectroscopic Observations of Initial Intermediates in the Photocycle of the Photoactive Yellow Protein from Ectothiorhodospira Halophila. *Biophys. J.* **1999**, *77*, 1017−1023.

(15) Gensch, T.; Gradinaru, C. C.; van Stokkum, I. H. M.; Hendriks, J.; Hellingwerf, K. J.; van Grondelle, R. The Primary Photoreaction of Photoactive Yellow Protein (PYP): Anisotropy Changes and Excitation Wavelength Dependence. *Chem. Phys. Lett.* **2002**, *356*, 347−354.

(16) Larsen, D. S.; van Stokkum, I. H. M.; Vengris, M.; van der Horst, M. A.; de Weerd, F. L.; Hellingwerf, K. J.; van Grondelle, R. Incoherent Manipulation of the Photoactive Yellow Protein Photocycle with Dispersed Pump-Dump-Probe Spectroscopy. *Biophys. J.* **2004**, *87*, 1858−1872.

(17) Larsen, D. S.; van Grondelle, R.; Hellingwerf, K. J. Primary Photochemistry in the Photoactive Yellow Protein: The Prototype Xanthopsin. In *Ultrashort Laser Pulses in Biology and Medicine*; Biological and Medical Physics Biomedical Engineering; Springer: Berlin, Heidelberg, 2008; pp 165−199.

(18) Zhu, J.; Paparelli, L.; Hospes, M.; Arents, J.; Kennis, J. T. M.; van Stokkum, I. H. M.; Hellingwerf, K. J.; Groot, M. L. Photoionization and Electron Radical Recombination Dynamics in Photoactive Yellow Protein Investigated by Ultrafast Spectroscopy in the Visible and Near-Infrared Spectral Region. *J. Phys. Chem. B* **2013**, *117*, 11042−11048.

(19) Xie, A.; Hoff, W. D.; Kroon, A. R.; Hellingwerf, K. J. Glu46 Donates a Proton to the 4-Hydroxycinnamate Anion Chromophore During the Photocycle of Photoactive Yellow Protein. *Biochemistry* **1996**, *35*, 14671−14678.

(20) Genick, U. K.; Soltis, S. M.; Kuhn, P.; Canestrelli, I. L.; Getzoff, E. D. Structure at 0.85 Å Resolution of an Early Protein Photocycle Intermediate. *Nature* **1998**, *392*, 206−209.

(21) Unno, M.; Kumauchi, M.; Sasaki, J.; Tokunaga, F.; Yamauchi, S. Resonance Raman Spectroscopy and Quantum Chemical Calculations Reveal Structural Changes in the Active Site of Photoactive Yellow Protein. *Biochemistry* **2002**, *41*, 5668−5674.

(22) Kukura, P.; McCamant, D. W.; Mathies, R. A. Femtosecond Stimulated Raman Spectroscopy. *Annu. Rev. Phys. Chem.* **2007**, *58*, 461−488.

(23) Brown, K. E.; Veldkamp, B. S.; Co, D. T.; Wasielewski, M. R. Vibrational Dynamics of a Perylene−Perylenediimide Donor−Acceptor Dyad Probed with Femtosecond Stimulated Raman Spectroscopy. *J. Phys. Chem. Lett.* **2012**, *3*, 2362−2366.

(24) Fujisawa, T.; Creelman, M.; Mathies, R. A. Structural Dynamics of a Noncovalent Charge Transfer Complex from Femtosecond Stimulated Raman Spectroscopy. *J. Phys. Chem. B* **2012**, *116*, 10453−10460.

(25) Kukura, P.; McCamant, D. W.; Yoon, S.; Wandschneider, D. B.; Mathies, R. A. Structural Observation of the Primary Isomerization in

Vision with Femtosecond-Stimulated Raman. *Science* **2005**, *310*, 1006−1009.
(26) Shim, S.; Dasgupta, J.; Mathies, R. A. Femtosecond Time-Resolved Stimulated Raman Reveals the Birth of Bacteriorhodopsin's J and K Intermediates. *J. Am. Chem. Soc.* **2009**, *131*, 7592−7597.
(27) Dasgupta, J.; Frontiera, R. R.; Taylor, K. C.; Lagarias, J. C.; Mathies, R. A. Ultrafast Excited-State Isomerization in Phytochrome Revealed by Femtosecond Stimulated Raman Spectroscopy. *Proc. Natl. Acad. Sci. U.S.A.* **2009**, *106*, 1784−1789.
(28) Frontiera, R. R.; Fang, C.; Dasgupta, J.; Mathies, R. A. Probing Structural Evolution along Multidimensional Reaction Coordinates with Femtosecond Stimulated Raman Spectroscopy. *Phys. Chem. Chem. Phys.* **2011**, *14*, 405−414.
(29) Imamoto, Y.; Ito, T.; Kataoka, M.; Tokunaga, F. Reconstitution Photoactive Yellow Protein from Apoprotein and P-Coumaric Acid Derivatives. *FEBS Lett.* **1995**, *374*, 157−160.
(30) Mihara, K.; Hisatomi, O.; Imamoto, Y.; Kataoka, M.; Tokunaga, F. Functional Expression and Site-Directed Mutagenesis of Photoactive Yellow Protein. *J. Biochem.* **1997**, *121*, 876−880.
(31) Kumauchi, M.; Hamada, N.; Sasaki, J.; Tokunaga, F. A Role of Methionine100 in Facilitating PYPM-Decay Process in the Photocycle of Photoactive Yellow Protein. *J. Biochem.* **2002**, *132*, 205−210.
(32) Shim, S.; Mathies, R. A. Development of a Tunable Femtosecond Stimulated Raman Apparatus and Its Application to B-Carotene. *J. Phys. Chem. B* **2008**, *112*, 4826−4832.
(33) Wilhelm, T.; Piel, J.; Riedle, E. Sub-20-Fs Pulses Tunable Across the Visible from a Blue-Pumped Single-Pass Noncollinear Parametric Converter. *Opt. Lett.* **1997**, *22*, 1494−1496.
(34) Shim, S.; Mathies, R. A. Generation of Narrow-Bandwidth Picosecond Visible Pulses from Broadband Femtosecond Pulses for Femtosecond Stimulated Raman. *Appl. Phys. Lett.* **2006**, *89*, 121124.
(35) McCamant, D. W.; Kukura, P.; Yoon, S.; Mathies, R. A. Femtosecond Broadband Stimulated Raman Spectroscopy: Apparatus and Methods. *Rev. Sci. Instrum.* **2004**, *75*, 4971−4980.
(36) Kim, M.; Mathies, R. A.; Hoff, W. D.; Hellingwerf, K. J. Resonance Raman Evidence That the Thioester-Linked 4-Hydroxycinnamyl Chromophore of Photoactive Yellow Protein Is Deprotonated. *Biochemistry* **1995**, *34*, 12669−12672.
(37) Pan, D.; Philip, A.; Hoff, W. D.; Mathies, R. A. Time-Resolved Resonance Raman Structural Studies of the pB' Intermediate in the Photocycle of Photoactive Yellow Protein. *Biophys. J.* **2004**, *86*, 2374−2382.
(38) Unno, M.; Kumauchi, M.; Tokunaga, F.; Yamauchi, S. Vibrational Assignment of the 4-Hydroxycinnamyl Chromophore in Photoactive Yellow Protein. *J. Phys. Chem. B* **2007**, *111*, 2719−2726.
(39) Chosrowjan, H.; Mataga, N.; Shibata, Y.; Imamoto, Y.; Tokunaga, F. Environmental Effects on the Femtosecond−Picosecond Fluorescence Dynamics of Photoactive Yellow Protein: Chromophores in Aqueous Solutions and in Protein Nanospaces Modified by Site-Directed Mutagenesis. *J. Phys. Chem. B* **1998**, *102*, 7695−7698.
(40) Mizuno, M.; Hamada, N.; Tokunaga, F.; Mizutani, Y. Picosecond Protein Response to the Chromophore Isomerization of Photoactive Yellow Protein: Selective Observation of Tyrosine and Tryptophan Residues by Time-Resolved Ultraviolet Resonance Raman Spectroscopy. *J. Phys. Chem. B* **2007**, *111*, 6293−6296.
(41) Premvardhan, L. L.; van der Horst, M. A.; Hellingwerf, K. J.; van Grondelle, R. Stark Spectroscopy on Photoactive Yellow Protein, E46Q, and a Nonisomerizing Derivative, Probes Photo-Induced Charge Motion. *Biophys. J.* **2003**, *84*, 3226−3239.
(42) Gromov, E. V.; Burghardt, I.; Hynes, J. T.; Köppel, H.; Cederbaum, L. S. Electronic Structure of the Photoactive Yellow Protein Chromophore: Ab Initio Study of the Low-Lying Excited Singlet States. *J. Photochem. Photobiol., A* **2007**, *190*, 241−257.
(43) Jha, K. N.; Bolton, G. L.; Freeman, G. R. Temperature Shifts in the Optical Spectra of Solvated Electrons in Methanol and Ethanol. *J. Phys. Chem.* **1972**, *76*, 3876−3883.
(44) Van Brederode, M. E.; Gensch, T.; Hoff, W. D.; Hellingwerf, K. J.; Braslavsky, S. E. Photoinduced Volume Change and Energy Storage Associated with the Early Transformations of the Photoactive Yellow Protein from Ectothiorhodospira Halophila. *Biophys. J.* **1995**, *68*, 1101−1109.
(45) Schotte, F.; Cho, H. S.; Kaila, V. R. I.; Kamikubo, H.; Dashdorj, N.; Henry, E. R.; Graber, T. J.; Henning, R.; Wulff, M.; Hummer, G.; et al. Watching a Signaling Protein Function in Real Time via 100-Ps Time-Resolved Laue Crystallography. *Proc. Natl. Acad. Sci. U.S.A.* **2012**, *109*, 19256−19261.